

Evaluation of Anti-Biofilm Formation Effect of Nickel Oxide Nanoparticles (NiO-NPs) Against Methicillin-Resistant Staphylococcus Aureus (MRSA)

Ahmed Mahdi Rheima^{1,*}, Mohammed F. Al Marjani², Mohammed Fadhil Aboksour² and Srwa Hashim Mohammed³

¹Department of Chemistry, College of Science, Wasit University, Kut, Iraq

²Department of Biology, College of Science, Mustansiriyah University, Baghdad, Iraq

³Department of Chemistry, College of Education, University of Garmian, Kalar, Iraq

(*) Corresponding author: arahema@uowasit.edu.iq

(Received: 22 March 2021 and Accepted: 16 August 2021)

Abstract

In this project, Nickel oxide nanoparticles (NiO-NPs) have been synthesized by a photolysis method and assessed for their anti-biofilm activity. It is a strategy that is simple and inexpensive. The morphology and the average particle size was investigated by scanning electron microscope (SEM), transmitted electron microscope (TEM) and the crystallite size was calculated by (XRD) analysis. The XRD studies support the existence of NiO-NPs with a high degree of crystallinity. Their nickel oxide particle size was found to be around 13-31 nm. Forty-two samples of medical waste from different hospitals in Baghdad were between 2nd to 12th of October / 2020. Bacterial isolation results recorded fifteen Staphylococcus aureus isolates. Well diffusion method was used to determine of methicillin resistance S. aureus (MRSA), in addition to using the *mecA* gene as a molecular method to detection of methicillin resistance gene, the results of these both methods showed that the MRSA percentage of these two methods were 53.3% and 73.4% in well diffusion method and PCR respectively. Results of MRSA biofilm formation illustrated that only four isolates (36.3%) hadn't the ability to produce biofilm by using microtiter plate assay (MTP). In contrast, the other isolates (63.7%) could produce biofilm and they were ranging from strong to weak biofilm formation. Antimicrobial activity of different concentrations of NiO-NPs (10, 20, 30, 50, and 100 µg/ml) showed ranging of inhibition zones starting from 0 to 13 mm. In comparison, the MIC concentration was 265 µg/ml (63.7%) of seven MRSA isolates and 530 µg/ml (36.4%) of four isolates. Detection of hemolysis activities of NiO-NPs against human red blood cells (RBCs) was done. The results illustrate that the hemolytic activity was 2.38%, 2.23%, 2.41%, and 2.69% corresponding to 0, 0.01, 0.1, and 1 mg/ml of NiO-NPs.

Keywords: Biofilm detection, Antibiofilm activity, NiO-NPs, *MecA*, MRSA, Metal oxide nanoparticles, Hemolysis activity.

1. INTRODUCTION

The high level of flexibility of material science and nanotechnology to arrange nanostructures of both shape and size may give a good opportunity to create and discover new drugs to use against microbes [1]. As a result, the synthesis of novel nanoparticles (NPs) of many metal oxides has gotten a lot of attention because of their unique chemical, physical, as well as biological properties [2]. Changing the size and the shape of NPs may be used to tune

their physical, chemical, and biological properties, which is most effective when manipulations are performed at the atomic level, and that thing will allow to use many types of metal oxides (such as Nickel) and nano-sized metals. Metal NPs and metal oxide NPs have been shown to have sufficient potential effect against bacteria [3]. Many metal oxide NPs have been shown to have biological properties that are superior to the parent metal's NPs. Metal

oxide nanoparticles have grabbed the scientific community's interest for this reason. [4]. Metal oxide nanoparticles are regarded to be a viable technique for treating bacterial biofilms since bacterial resistance mechanisms that are effective against antibiotics cannot be used against NPs[5]. Nanoparticle interactions with bacterial cells or biofilms are governed by two driving factors: electrostatic and hydrophobic. Electrostatic NP interactions with microbes have been observed in a variety of settings. Positively charged (NP) molecules, especially those with a zeta potential larger than +40 mV, function as detergents on bacterial cell membranes, causing osmotic damage and ultimately cell death. On the other hand, the impact of NP with a low positive potential or those that are negatively charged is minimal or non-existent. [6]. Moreover, nickel oxide (NiO) has been proposed for use in many applications, like photovoltaic, gas sensing, emitting of light, among others [2-3].

Biofilm consists of a complex biochemical mix of polysaccharides, glycolpeptides, proteins, lipids and nucleotides that are generated in contact between the culture of microorganisms and extracellular matrix of polymers [7]. The main goal of biofilm is to shield bacteria from harmful environmental elements such as temperature, dryness, UV radiation, and immune factors [8].

Recently, antibacterial agents have been delivered using innovative nanotechnology-based antimicrobials to destroy planktonic bacteria, antibiotic-resistant species, and biofilm structures. Furthermore, improved anti-biofilm activities were reported when compounds' anti-biofilm activity was combined with the specific features of NPs or functionalized surfaces with NPs [9].

The importance of biofilm is appearing if we know that the antibiotic doses needed to kill or inhibit bacteria are 1000 times lower than the concentration required to fully eliminate biofilm [10].

Staphylococcus aureus (*S. aureus*) represents one of the common pathogenic bacteria around the world; it can develop

mechanisms of resistance to use it against a wide range of antibiotics since discovering and using penicillin as a first effective antibiotic [11]. Penicillin acts by inhibiting a protein called penicillin-binding protein (PBP), which is essential for bacteria's cell wall synthesis, and that will lead to killing the bacterial cells as a result of osmosis [12-13]. Soon after that, bacteria began to produce penicillinase enzyme (as a type of β -lactamase enzyme), that enzyme can destroy the penicillins and give the resistance characteristics to that antibiotic [11-14]. The last bacterial mechanism led to producing penicillinase-resistant semisynthetic penicillin called methicillin. Methicillin has a similar working mechanism to penicillin, except for an additional methoxy group that creates an enzyme that decreases the affinity for staphylococcal β -lactamase [14-15]. *S. aureus*, on the other hand, soon evolved resistance to methicillin and then became known as methicillin-resistant *S. aureus* [14].

The current study aims to determine the characteristics of nickel oxide nanoparticles (NiO-NPs) and their antimicrobial effect against methicillin resistance *S. aureus* (MRSA), furthermore, its antibiofilm formation process of bacterial isolates, as well as its hemolytic effects against RBCs which was used to assess NiO-NPs' biocompatibility as a possible candidate.

2. EXPERIMENTAL

2.1. Synthesis of Nickel Oxide Nanoparticles (NiO-NPs)

Nickel nitrate $\text{Ni}(\text{NO}_3)_2$, Ethylene glycol $(\text{CH}_2\text{OH})_2$, de-ionized water has been used in this research, All chemical products were bought from (BDH) and not cleaned. NiO-NPs have been prepared by photolysis method [16-17], an irradiation cell was utilized to irradiate nickel salt source to produce NiO-NPs, as seen in Figure 1. The lamp has been selected with a maximum light intensity of UV mercury (125 W) at 365nm. The cell contains a quartz tube as a UV immersion jacket in nickel salt solution.

Pyrex is a simple way for a reactor to be used. The reactor is refrigerated with an ice bath to prevent an increase in temperature. Accordingly, 0.01 mole of nickel nitrate $\text{Ni}(\text{NO}_3)_2$ was dissolved in a 100 ml de-ionized water; then, 100 ml of 0.01 mole Ethylene glycol was added gradually to the solution with stirred for 1 h. The solution was irradiated for 30 minutes, and a light green precipitate was formed. The samples were separated and passed through a centrifuge many times washing by de-ionized water. At the end of one day draining, the sample was calcined on an oven at 400°C for 3 h to create a pure black-brown stable precipitate of nickel oxide nanoparticles. .



Figure 1. Photocell of Synthesis NiO-NPs

2.2. Characterization of NiO-NPs

The sample of NiO-NPs was mounted on a glass slide, X-ray diffraction was performed using (XRD-6000) at 30 mA and 40 kV to produce x rays at a wavelength of 1.54 \AA . transmission electron microscopy (TEM) type JEOL JEM-2100 was used to investigate the size and morphology of nanoparticles. Scanning electron microscope (SEM) type JEOL JEM-6510 LV to investigated the dimensions of the NiO-NPs [18-19].

2.3. Bacterial Isolates and Growth Conditions

Forty-two samples of medical waste of different hospitals in Baghdad were in the period between 2nd to 12th of October / 2020. All isolates were identified according

to their microscopic characteristics, in addition to other biochemical results such as catalase, coagulase, DNase, gelatinase hydrolysis, and mannitol fermentation tests, as well as using the VITEK2 system to confirm the bacterial identification.

2.4. Methicillin Resistance S. Aureus Detection

Both oxacillin disc diffusion and cefoxitin disc diffusion were performed of all *S. aureus* isolates [20-21], as well as growth on CHROMagar, ATCC 29213 was used as a negative control strain which is methicillin sensitive *S. aureus* (MSSA). Susceptibility of bacterial isolates against oxacillin and cefoxitin antibiotic discs was performed by using oxacillin disc ($1 \mu\text{m}$) and cefoxitin discs (30 mg). Suspension of all bacterial isolates were done and adjusted equal to 0.5 McFarland, $100 \mu\text{l}$ of each bacterial suspensions were cultured on Mueller–Hinton agar plate, then both oxacillin and cefoxitin antibiotic discs were plated separately on the plate. After incubation at 37°C for 18 hrs, the inhibition zone were determined and compared with diameter zone which identified according to CLSI [22].

2.5. Bacterial DNA Preparation

Bacterial DNA of the collected isolates was extracted by using the boiling method [23-24], single colonies of isolates transferred in $100 \mu\text{l}$ of distilled sterilized water and mixed by using a vortex. Then, the suspensions were boiled for twenty minutes, centrifuged at (8000 rpm) for 2 mint, and then the supernatants of all tubes were transferred to new sterilized eppendorf tubes separately and considered as the bacterial DNA template and used for PCR detection.

2.6. PCR Detection of mecA gene

Detection of *mecA* gene was done by using primers which are described in many previous studies [23]. *mecA*F: 5-GTAGAAATGACTGAACGTCCGATAA-3 and *mecA* R: 5-CCAATTCCACATT

GTTCGGTCTAA-3 (310 bp.). Five μl of the DNA template of each isolated was transferred separately to 1.5 ml eppendorf tubes containing 10 μl of master mix (Jena, Germany), 1.5 μl of both forward and reverse mecA primers, 2 μl of deionized sterilized water to reach to final volume equal to 20 μl . The PCR operating experience was designed to include three main steps, the first step including heating the machine to 96° for 4 min, followed by 35 cycles of step two which can be subdivided into three steps; denaturation (96° for 30 sec), annealing (64° for 30 sec), and elongation (72° for 45 sec), finally the third main step include keeping the test in 72° for 5 minutes.

2.7. Determination of Bacterial Biofilm Formation Assay

Biofilm formation was performed by the Microtiter plate (MTP) assay as previously described [25]. Briefly, MRSA isolates were grown overnight in brain-heart infusion broth at 37 degrees. The bacterial culture was diluted to achieve ($\text{OD}_{595} = 0.137$). After that, (20 μl) of bacterial growth was added to inoculate microtiter plates containing (80 μl) of Brain Heart Infusion broth (BHIB) with 2% sucrose, and then incubated for 24 hours at 37 degrees. After washes two times with PBS and left to be dried at room temperature. Unattached bacterial cells were removed. 200 μl of solution of 0.1% (w/v) crystal violet was used for Biofilm staining. Next, the crystal violet bound to the adherent bacterial cells was disposed of with 200 μl of ethyl alcohol (95%), and the wells were rewashed with (PBS) and left to be dried at room temperature. The optical density (OD) values of all isolates were determined by ELISA (enzyme-linked immunosorbent assay) reader at (630 nm). This test was done in triplicate, the biofilm formation controls were bacterial cultures. However, the bacterial biofilm results were recorded and classified into four groups according to comparison with the cut-off OD value (OD_c) which represents the mean optical

density of the broth only as a negative control. The first group mentioned as no biofilm formation and contains isolates which their $\text{OD} \leq \text{OD}_c$, the second group mentioned as weak biofilm formation and contains bacterial isolates which their OD more than OD_c and less than double value of it, $\text{OD}_c < \text{OD} \leq (2 \times \text{OD}_c)$, the third group contains moderate biofilm former isolates, which their OD more than double OD_c and less than OD_c multiply by four, $(2 \times \text{OD}_c) < \text{OD} \leq (4 \times \text{OD}_c)$, while the final group contains high biofilm former isolates with OD more than OD_c multiply by four, $(4 \times \text{OD}_c) < \text{OD}$.

2.8. Determination of NiO-NPs Effects on Biofilm Assay

Effect of Ni-NPs against biofilm formation of the MRSA was performed by the same procedure described above, with adding 100 μl different concentrations of Ni-NPs (15.62, 31.25, 62.5, 125, 250, and 500 $\mu\text{g}/\text{ml}$) in each well to determine the NiO-NPs anti-biofilm activity. The rate of inhibition generated by (NiO-NPs) was calculated using the formula below.

Inhibition rate (%) = $(\text{Control OD}_{595} - \text{Treated OD}_{595}) / (\text{Control OD}_{595}) \times 100$

2.9. Antibacterial Activity of NiO-NPs

The antibacterial activity of NiO-NPs against MRSA isolates was detected using agar well diffusion method as per CLSI guidelines using 10, 20, 30, 50, and 100 $\mu\text{g}/\text{ml}$ of NiO-NPs, in addition to using sterilized distilled water as a negative control [26]. The (MIC) of nanoparticles was measured by resazurin-based turbidometric [27]. Briefly, in a microtiter plate with 96-well, 100 μl of nutrient broth was added to each well, and then 100 μl of NiO nanoparticles (10000 $\mu\text{g}/\text{ml}$) was added to 1st vertical row from A1 to A10 and mixed. After that, a micropipette tip was used to add 100 μl of the suspension in the first well to the second one in the same line. Then, from second well to the third well, 100 μl of the suspension was transferred and mixed. The dilution was

done till the 8th well serially, and 100µl was lastly transferred from the last well and discarded. Finally, five µl of MRSA suspension (1×10^6 CFU/ml) was added into all wells (except the row A11-H11 as negative control). 24h after, 10 µl of resazurin was added to each well and, incubated for 4 h at 37degrees Celsius. Additionally, the effect of different concentrations of NiO NPs. (0.625, 1.25, 2.5, 5, and 10 µg/ml) was examined against isolates (n=7) using an Ultraviolet–visible spectroscopy every two hours to evaluate the antibacterial effect of increased concentrations of NiO-NPs on MRSA.

2.10. Detection of Hemolytic Activity of NiO-NPs.

Detection of hemolysis activity of NiO-NPs was performed according to Morteza et al. [28], ten ml of blood cells was put into anti-agglutinated tubes (contain EDDA) and then the tube was centrifuged at 3000 rpm for 10 min, phosphate buffer saline (PBS) was used to wash the precipitate twice and erythrocytes were suspended in 10% of PBS (v/v). 100 µl of the ten-fold of the last suspension were transferred to 1.5 ml Eppendorf tubes containing different concentrations of Ni-NPs (10, 100, and 1000) µg/ml. after incubation at 37° for 150 min, the Eppendorf tubes were centrifuged at (3000 rpm) for five min and the absorbance of the hemoglobin of the tubes was measured at 580 nm by using spectrophotometer, positive and negative controls were prepared by adding diluted RBCs with distilled water and PBS respectively. Finally, the percentage of hemolysis RBCs was calculated by using the following formula:

$$\text{Hemolysis (\%)} = \frac{(\text{Absorption of samples} - \text{Absorption of negative control})}{(\text{Absorption of positive control} - \text{Absorption of negative control})}$$

3. RESULTS AND DISCUSSION

The X-ray diffraction patterns of photo-chemically (NiO-NPs) synthesized illustrates in Figure 2. The result of X-ray

diffraction analysis shows NiO Nano-powder has a cubic structure (JCPDS 00-047-1049). The peaks are located at an angle of 2θ at (37.2, 43.5, 63.0, 75.3 and 79.5) which refer to the 111, 200, 220, 311 and 222 plane of the cubic structure of (NiO-NPs). By measuring the XRD, we observe a high purity of the prepared sample and the brooding peaks indicates a decrease in size, which confirms the formation of particles at the nanoscale. The average crystallite size was estimated as 11.17 nm by Debye-Scherrer formula.

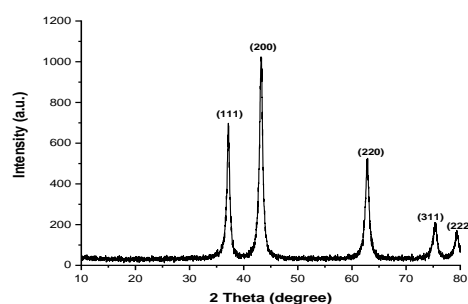


Figure 2. XRD pattern of NiO Nanoparticles.

TEM images have been reported to forecast the photochemical produced photo morphology and size of synthesized (NiO-NPs), as shown in Figures 3a and b. It can be shown that the substance consists of cubical particles of approximately 13–31 nm. It fits with the evaluation of Scherrer's formula data. TEM pictures also prove that the prepared Nano-samples are free of any lumps and clusters. All sizes formed are less than 100 nanometers, and this indicates that the created sample is zero-dimensional. Typical SEM images are shown in Figures (4 a and b) for the Nano-synthesized NiO. The SEM image of the precursor NiO NPs shows smooth and uniform particle morphology with a non-spherical particle shape with average particles size almost equal to 17.65 nm. We see that the average particle size measured by TEM and SEM values is in good accordance with the average size of crystal predicted by the Scherrer equations from the XRD pattern.

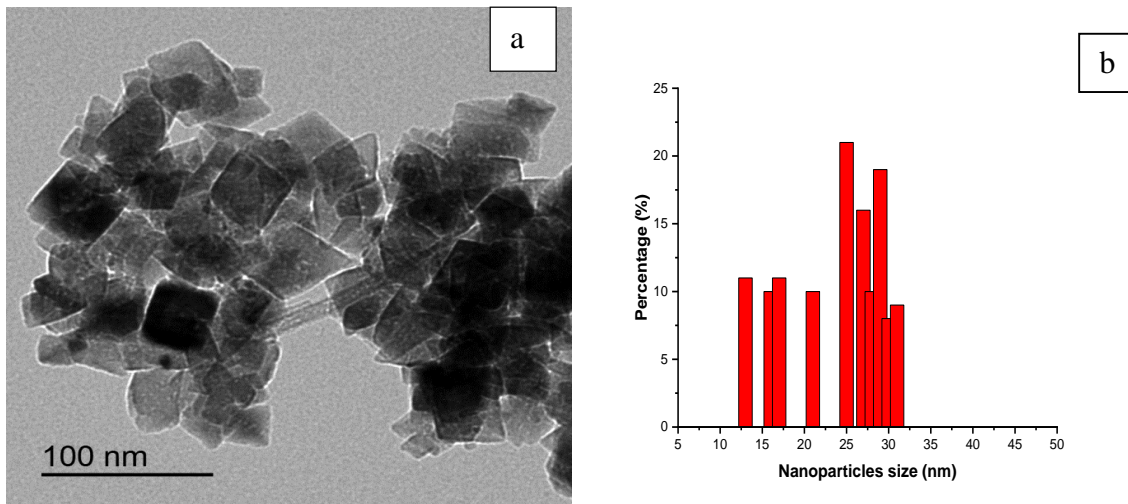


Figure 3. (a) TEM image of NiO Nano-synthesized. (b) TEM NPs Distribution.

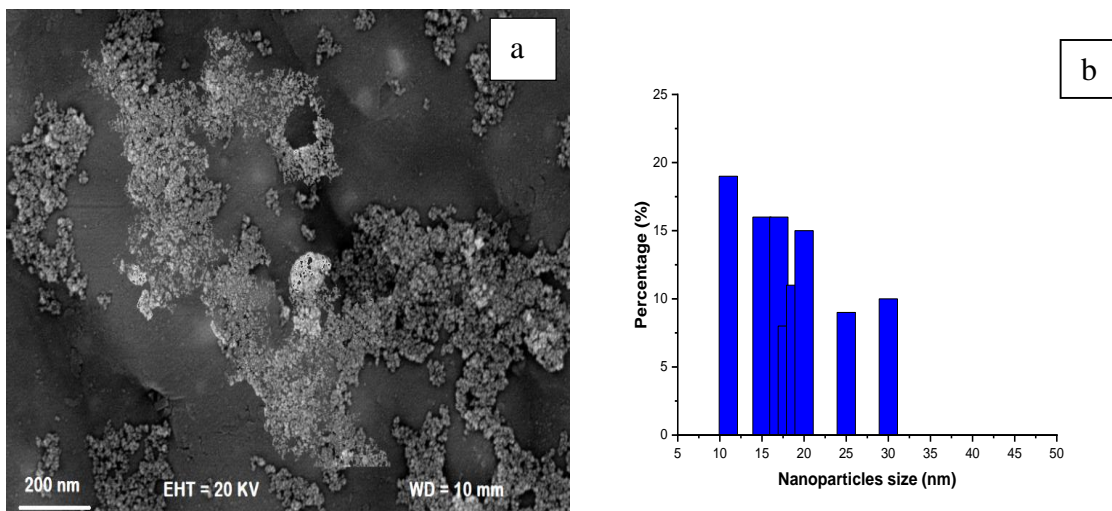


Figure 4. (a) SEM image of NiO Nanoparticles. (b) SEM nanoparticles distribution.

Bacterial identification results showed that out of forty-two samples of the medical waste collected; fifteen *S. aureus* isolates were identified, with isolation percentage were equal to 35.7%. All these isolates were blue color as Gram positive small round bacteria (cocci) and they tend to be aggregated in groups like clusters. The results of biochemical tests illustrated the ability of bacterial isolates to produce catalase, gelatinase, DNase, and coagulase enzymes, while it gives a negative result in the oxidase enzymes test. Results of methicillin resistance of bacterial isolates showed that eight *S. aureus* isolates (53.3%) out of fifteen isolates mentioned as MRSA, recorded inhibition zone ≥ 13 mm and ≥ 22

mm in oxacillin and cefoxitin disc diffusion methods respectively. MRSA represents a serious problem in all hospitals, health care organizations, and clinical centers, and the early identification of these bacteria may strongly help in the treatment of these cases. [29] MRSA is easily spread in all parts of the environment by contact with carrier or infected people, and it can make a serious skin infection starting with bump, red, and swollen areaa, as well as many other morbidity syndromes, which may reach to high percentage of mortality. [30] On the other hand, results of *mecA* gene detection, showed that eleven *S. aureus* isolates (73.4%) contain *mecA* gene and mentioned as MRSA, as shown in figure 5. The

difference between the two percentages of methicillin resistance *S. aureus* isolates in disc diffusion and PCR methods (which were 53.3% and 73.4% respectively) referred to the high resolution of PCR technique than disc diffusion method, which was recorded in many previous studies [21].

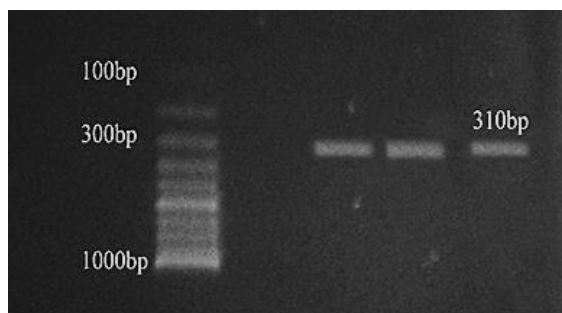


Figure 5. *mecA* gene in MRSA isolates

According to biofilm formation results, the cutoff value of OD recorded as 0.214 which was similar to OD of negative control, so four isolates (36.3%) were mentioned as non-forming biofilm bacteria since their OD values less than 0.214, while three isolates of MRSA (27.2%) recorded OD values more than 0.856 and mentioned as strong biofilm former bacterial isolates, finally two groups of bacterial isolates (18.2%) (Two isolates in each group) recorded as moderate biofilm former isolates and weak biofilm former isolates based on their OD values which were between 0.428-0.856, and 0.214 -0.428 respectively. The results showed that seven isolates (63.7%) out of eleven MRSA isolates were biofilm formation; these results strongly refer to the importance and wide distributions of biofilm formation among MRSA as recorded in many types of research [31].

The results of anti-biofilm formation activity of NiO-NPs illustrated decreasing of OD when Ni-NPs concentrations were increased, OD was recorded at 0.491 with the absence of NiO-NP, 0.463 with the presence of (15.6 µg/ml) of Nickel-NPs,

0.447 with presence of (31.25 µg/ml) of Nickel-NPs, and then starting to decrease till it reached to 0.081 with the presence of 0.5 mg of Ni-NPs, see figure 6. Furthermore, the effects of Ni-NPs were significant ($P < 0.05$) to concentrations 62.5, 125, 250, and 500 µg/ml.

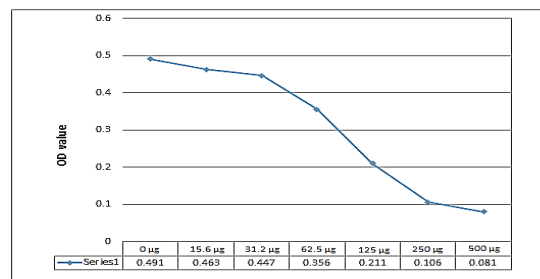


Figure 6. The production of MRSA biofilms in the influence and absence of Nickel oxide-NPs

Detection of the agar-well diffusion method was used to test the antibacterial activity of Nickel oxide Nanoparticles (NiO NPs) was ranging between non to small inhibition zone; which were reaching 13 mm in two MRSA isolates, 11 mm in three isolates, 8 mm in three isolates as the effect of 100 µg/ml of NiO-NPs without any recording zone to the other selected concentrations of NiO-NPs, while the other isolates didn't record any inhibition zone of all the tested NiO-NPs concentrations. Moreover, the results of MIC values of NiO-NPs illustrated that the values were ranging between 250 - 500 µg/ml of Ni-NPs, as indicated in table 1. The antibacterial effect of particles is influenced by their size, and most investigations have shown that antibacterial activity increases as particle size decreases [32]. Because produced

NiO-NPs have a smaller particle size, they adhere to the cellular membrane quickly by electrostatic contact. This contact initiates oxidative stress, which results in the creation of free radicals (ROS) [33].

Table 1. MIC values of NiO-NPs concentrations.

MIC value	NiO-NPs concentration (µg/ml)										
	1060	530	265	128	64	32	16	8	4	2	1
No. of isolate	-	4	7	-	-	-	-	-	-	-	-
Percentage %	-	36.4	63.7	-	-	-	-	-	-	-	-

Detection of the hemolytic effect of NiO-NPs illustrated the hemolytic activity of nickel nanoparticles on human RBC was 2.38%, 2.23%, 2.41%, and 2.69% as a result corresponding to 0, 0.01, 0.1, and 1 mg/ml of NiO-NPs, as shown in figure 7. Hemolysis is characterized by the release of hemoglobin into the plasma as a result of erythrocyte membrane injury. The hemolytic test represents an indicator of in vivo toxicity of the tested sample. As-synthesized NiO-NPs were found to be less toxic to RBCs even with using a high concentration of NiO-NPs which was reached to 1000 µg/ml. Also, significant hemolysis deference wasn't achieved as a result of NiO NPs effects.

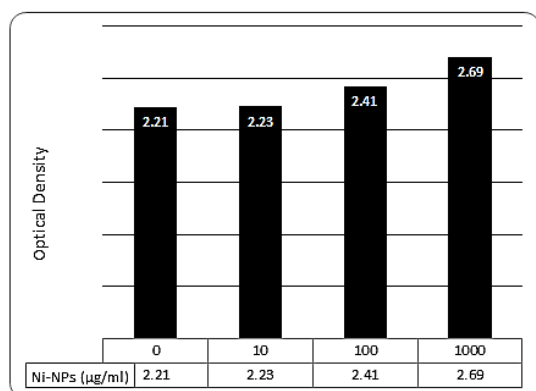


Figure 7. Effects of NiO-NPs on human RBCs hemolysis.

The electrostatic interaction of bacterial membrane components with negative charges and the positive charged nanoparticles could explain the antibacterial effect of biologically manufactured NiO-NPs. [34]. Ni²⁺ NPs can penetrate the cell wall, causing damage

to cellular proteins and DNA, as well as interrupting the electron transport chain (ETC), resulting in cell content leakage and, eventually, organism death. [35].

4. CONCLUSIONS

To improve bactericidal activity, NiO-NPs were successfully synthesized by a photolysis method. The synthesized NiO-NPs show a high degree of crystallinity with an average particle size around 13 to 31 nm which is calculated by transmitted electron microscope (TEM). These sizes of particles give them preference in medical applications. The effective role of the NiO-NPs against bacterial growth and biofilm formation was assessed against MRSA. Overall, the current study was indicated that nanoparticles in vitro they exhibit high antibacterial and antibiofilm properties.

Lastly, in an era where Methicillin-resistant *Staphylococcus aureus* (MRSA) is on the rise, fighting infectious infections and curing patients is becoming increasingly challenging, resulting in significant morbidity and mortality. NiO-NPs appear to have a strong potential to solve the emergence of bacterial MRSA and are a feasible alternative to antibiotics.

ACKNOWLEDGEMENT

To everyone who helped us complete this project, specifically at Al- Mustansiriyah University, Wasit University and Garmian University.

CONFLICT OF INTEREST

The authors declare that they have no conflict of interest.

REFERENCES

1. Heydari, S., Shirmohammadi Aliakbarkhani, Z., "Photocatalytic Degradation of Safranin Dye from Aqueous Solution Using Nickel Nanoparticles Synthesized by Plant Leaves", *International Journal of Nanoscience and Nanotechnology*, 6(3) (2020) 153-165.
2. John, T., Parmar, K. A., Kotval, S. C., Jadhav, J., "Synthesis, Characterization, Antibacterial and Anticancer Properties of Silver Nanoparticles Synthesized from Carica Papaya Peel Extract", *International Journal of Nanoscience and Nanotechnology*, 17(1) (2021) 23-32.
3. Mokoena, T. P., Swart, H. C., Motaung, D. E., "A review on recent progress of p-type nickel oxide based gas sensors: Future perspectives", *Journal of Alloys and Compounds*, 805 (2019) 267-294.
4. Stankic, S., Suman, S., Haque, F., Vidic, J., "Pure and multi metal oxide nanoparticles: synthesis, antibacterial and cytotoxic properties", *Journal of Nanobiotechnology*, 14 (2016) 1-20.
5. Chen, S. C., Kuo, T. Y., Lin, H. C., Chen, R. Z., Sun, H., "Optoelectronic properties of p-type NiO films deposited by direct current magnetron sputtering versus high power impulse magnetron sputtering", *Applied Surface Science*, 508 (2020) 145106.
6. Diab, R., Khameneh, B., Joubert, O., Duval, R., "Insights in nanoparticle-bacterium interactions: new frontiers to bypass bacterial resistance to antibiotics", *Current pharmaceutical design*, 21 (2015) 4095-4105.
7. Abidi, S. H., Sherwani, S. K., Siddiqui, T. R., Bashir, A., Kazmi, S. U., "Drug resistance profile and biofilm forming potential of *Pseudomonas aeruginosa* isolated from contact lenses in Karachi-Pakistan.", *BMC ophthalmology*, 13(1) (2013) 1-6 .
8. Han, C., Romero, N., Fischer, S., Dookran, J., Berger, A., Doiron, A. L., "Recent developments in the use of nanoparticles for treatment of biofilms", *Nanotechnology Reviews*, 6.5 (2017) 383-404.
9. Malaekheh-Nikouei, B., Bazzaz, B. S. F., Mirhadji, E., Tajani, A. S., Khameneh, B., "The role of nanotechnology in combating biofilm-based antibiotic resistance", *Journal of Drug Delivery Science and Technology*, (2020) 101880.
10. Lobanovska, M., Pilla, G., "Focus: drug development: Penicillin's discovery and antibiotic resistance: lessons for the future?", *The Yale journal of biology and medicine*, 90 (2017) 135.
11. Stapleton, P. D., Taylor, P. W., "Methicillin resistance in *Staphylococcus aureus*: mechanisms and modulation", *Science progress*, 85 (2002) 57-72.
12. Chambers, H. F., DeLeo, F. R., "Waves of resistance: *Staphylococcus aureus* in the antibiotic era", *Nature Reviews Microbiology*, 7 (2009) 629-641.
13. Kallen, A. J., Mu, Y., Bulens, S., Reingold, A., Petit, S., Gershman, K. E. N., Ray, S. M., Harrison, L. H., Lynfield, R., Dumyati, G., Townes, J. M., "Health care-associated invasive MRSA infections, 2005-2008", *Jama*, 304 (2010) 641-647.
14. Cooke, F. J., Brown, N. M., "Community-associated methicillin-resistant *Staphylococcus aureus* infections", *British medical bulletin*, 94 (2010) 215-227.
15. Mohammed, M. A., Rheima, A. M., Jaber, S. H., Hameed, S. A., "The removal of zinc ions from their aqueous solutions by Cr₂O₃ nanoparticles synthesized via the UV-irradiation method", *Egyptian Journal of Chemistry*, 63 (2020) 425-431.
16. Kamil, A. F., Abdullah, H. I., Mohammed, S. H., "Cibacron red dye removal in aqueous solution using synthesized CuNiFe₂O₅ Nanocomposite: thermodynamic and kinetic studies", *Egyptian Journal of Chemistry*, 12 (2021) 18-24.
17. Rheima, A., Anber, A. A., Shakir, A., Salah Hammed, A., Hameed, S., "Novel method to synthesis nickel oxide nanoparticles for antibacterial activity", *Iranian Journal of Physics Research*, 20 (2020) 51-55.
18. Kamil, A. F., Abdullah, H., Rheima, A. M., Mohammed, S. H., "Photochemical synthesized NiO nanoparticles based dye-sensitized solar cells: a comparative study on the counter electrodes and dye-sensitized concentrations", *Journal of Ovonic Research*, 17 (2021) 299-305.
19. Otter, J. A., French, G. L., "Bacterial contamination on touch surfaces in the public transport system and in public areas of a hospital in London", *Letters in Applied Microbiology*, 49 (2009) 803-805 .
20. Roberts, M. C., Soge, O. O., No, D., Beck, N. K., Meschke, J. S., "Isolation and characterization of methicillin-resistant *Staphylococcus aureus* from fire stations in two northwest fire districts", *American Journal of Infection Control*, 39 (2011) 382-389 .
21. Sekar, R., Srivani, S., Amudhan, M., Mythreyee, M., "Carbapenem resistance in a rural part of southern India: *Escherichia coli* versus *Klebsiella spp*", *The Indian journal of medical research*, 144 (2016) 781-785.
22. Nacheervan, M. G., "Virulence potential of *S. aureus* isolated from imported and local chicken depending on the phenol soluble modulins in Duhok Iraq", *Bas. J. Vet. Res.*, 2 (2002) 103-115 .
23. "Abo-Ksour, M. F., "Presence of Extended-Spectrum?-Lactamases Genes in *E. coli* Isolated from Farm Workers in the South of London", *International Journal of Pharmaceutical Quality Assurance*, 9(1) (2018) 64-67 .

24. Badmasti, F., Siadat, S. D., Bouzari, S., Ajdary, S., Shahcheraghi, F., “Molecular detection of genes related to biofilm formation in multidrug-resistant *Acinetobacter baumannii* isolated from clinical settings”, *Journal of Medical Microbiology*, 64(5) (2015) 559-564.
25. Heatley, N. G.,” “A method for the assay of penicillin”, *Biochemical Journal*, 38 (1944) 61-65.
26. Teh, C. H., Nazni, W. A., Norazah, A., Lee, H. L., “Determination of antibacterial activity and minimum inhibitory concentration of larval extract of fly via resazurin-based turbidometric assay”, *BMC Microbiology*, 17 (2017) 1-8.
27. Vahedi, M., Hosseini-Jazani, N., Yousefi, S., Ghahremani, M., “Evaluation of anti-bacterial effects of nickel nanoparticles on biofilm production by *Staphylococcus epidermidis*”, *Iranian Journal of Microbiology*, 9(3) (2017) 160-172.
28. Houston, P., Rowe, S. E., Pozzi, C., Waters, E. M., O’Gara, J. P., “Essential role for the major autolysin in the fibronectin-binding protein-mediated *Staphylococcus aureus* biofilm phenotype”, *Infection and immunity*, 79(3) (2011) 1153-1165.
29. Geoghegan, J. A., Corrigan, R. M., Gruszka, D. T., Speziale, P., O’Gara, J. P., Potts, J. R., Foster, T. J., “Role of surface protein SasG in biofilm formation by *Staphylococcus aureus*”, *Journal of Bacteriology*, 192(21) (2010) 5663-5673.
30. Abo-Ksour, M. F., Al-Jubori, S. S., Jawad, H. A., “Influence of Helium-Neon Laser on Some Virulence Factors of *Staphylococcus Aureus* and *Escherichia Coli*”, *Al-Mustansiriyah Journal of Science*, 29(3) (2019) 29-34.
31. Aziz, S. N., Al Marjani, M. F., Rheima, A. M., Al Kadmy, I. M., “Antibacterial, antibiofilm, and antipersister cells formation of green synthesis silver nanoparticles and graphene nanosheets against *Klebsiella pneumoniae*”, *Reviews in Medical Microbiology*, 24 (2021) 25-36.
32. Jasim, N. A., Al-Gasha'a, F. A., Al-Marjani, M. F., Al-Rahal, A. H., Abid, H. A., Al-Kadhmi, N. A., Jakaria, M., Rheima, A. M.,” “ZnO nanoparticles inhibit growth and biofilm formation of vancomycin-resistant *S. aureus* (VRSA)”, *Biocatalysis and Agricultural Biotechnology*, 29 (2020) 101745.
33. Ezhilarasi, A. A., Vijaya, J. J., Kaviyarasu, K., Maaza, M., Ayeshamariam, A., Kennedy, L. J., “Green synthesis of NiO nanoparticles using *Moringa oleifera* extract and their biomedical applications: Cytotoxicity effect of nanoparticles against HT-29 cancer cells”, *Journal of Photochemistry and Photobiology B: Biology*, 164 (2016) 352-360.
34. Basak, G., Das, D., Das, N., “Dual role of acidic diacetate sophorolipid as biostabilizer for ZnO nanoparticle synthesis and biofunctionalizing agent against *Salmonella enterica* and *Candida albicans*”, *Journal of Microbiology and Biotechnology*, 24 (2014) 87-96.
35. Wong, K. K., Liu, X., “Silver nanoparticles the real silver bullet in clinical medicine?”, *Med. Chem. Comm.*, 1(2) (2010) 125-131.